Update on AMR and Implicit MHD

Ravi Samtaney
samtaney@pppl.gov
http://www.pppl.gov/APDEC-CEMM/

Computational Plasma Physics Group
Princeton Plasma Physics Laboratory
Princeton University

CEMM Meeting, Boulder CO,
March 30, 2008

PPPL
PRINCETON PLASMA PHYSICS LABORATORY

Outline

- AMR-MHD
  - *Level-set method for poloidal planes*
  - *Results of pellet injection simulations*
- Implicit Newton-Krylov Method for MHD
  - *Wave-structure based preconditioner*

“Shaped” Plasma Cross-section

- Structured mesh approaches to handle “shaped” plasma cross-sections
  - *Mapped grids in poloidal plane*

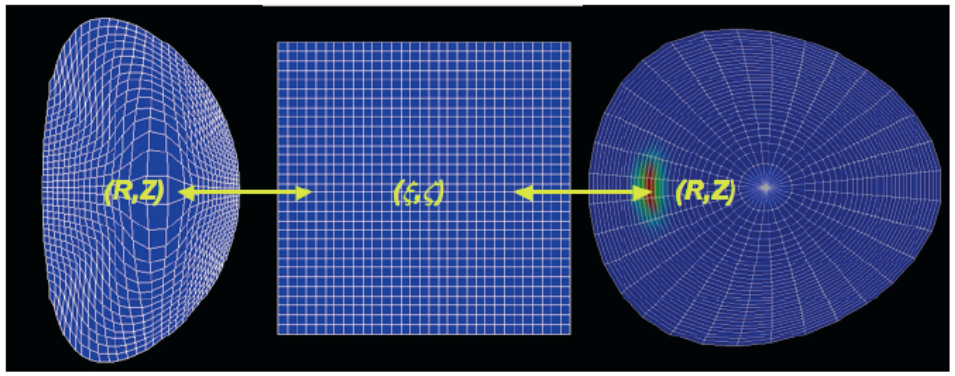

- Embedded boundary approach
  - *Cut-cells*
- Level-set approach
  - *No cut-cells*
  - *Boundary representation is implicit*

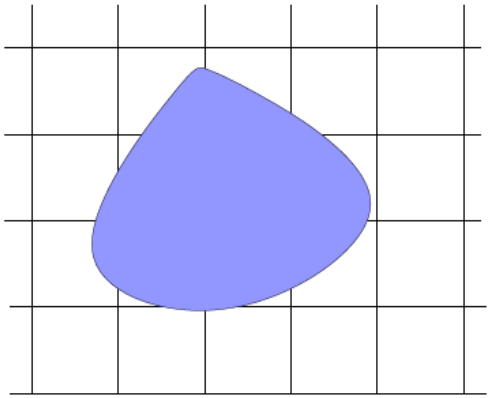

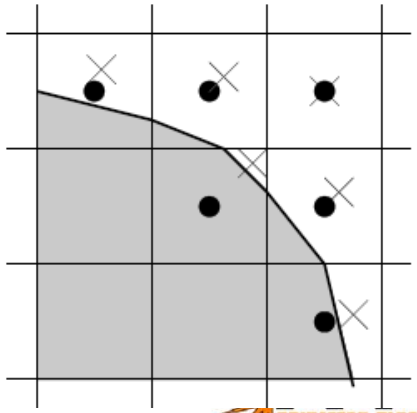

PRINCETON PLASMA PHYSICS LABORATORY

Cartesian Grid Representation of Irregular Boundaries

- History
  - *Shortley & Weller (1938) - Poisson equation on irregular geometries*
  - *Richtmyer & Morton (1964) - track moving fronts using polygonal representation*
  - *Noh (1964) - overlapping Lagrangian-Eulerian grid methods for material interfaces*
  - *With AMR: Chern & Colella (1987), Bell, Colella & Welcome (1991)*
  - *Embedded boundary AMR: Colella & Applied Numerical Algorithms Group at LBL (ongoing work under SciDAC funding)*
- Level-Set Approach
  - *Original idea by Osher & Sethian (1988)*
  - *Mulder, Osher & Sethian (1992) - for interface tracking compressible gas dynamics*
  - *Fedkiw et al. (1999) - for multi-material interfaces (ghost fluid method)*
  - *Arienti et al. (2003) - Eulerian - Lagrangian coupling in fluid-solid interactions*
  - *Aslam (2003) - Multidimensional extrapolation using a PDE approach*
  - *Many others - see review paper by Osher & Fedkiw (2001)*

Level-set Approach

- Advantages
  - *Most computations done on a regular grid - efficiency, accuracy*
  - *Grid generation is tractable*
  - *For moving or free boundaries the motion of the grid does not affect the regularity of the grid away from the boundary*
  - *No coordinate singularities or large variation in metric terms to contend with*
  - *Geometric multi-grid for elliptic solvers*
  - *Local refinement*
- Disadvantages
  - *Boundary representation is implicit*
  - *Mesh not aligned with flux surfaces*
  - *Conservation to machine accuracy is not fulfilled*
  - *Generally lower order of accuracy at boundary - unsuitable for problems with boundary layers*
  - *Requires more theory particularly stability theory*

Level-set Approach for Tokamak MHD

- Adopt the level-set approach to handle shaped poloidal cross-section
  - *Underlying grid is Cartesian*
  - *For now the boundary is fixed*
- Basic Idea
  - *"Ghost cells" are commonly used in regular grid computations to impose boundary conditions*
  - *Generalize the above idea to have a "ghost fluid region"*
  - *Extrapolate variables from the "real fluid region" to the ghost region such that physical (& numerical) boundary conditions are satisfied*

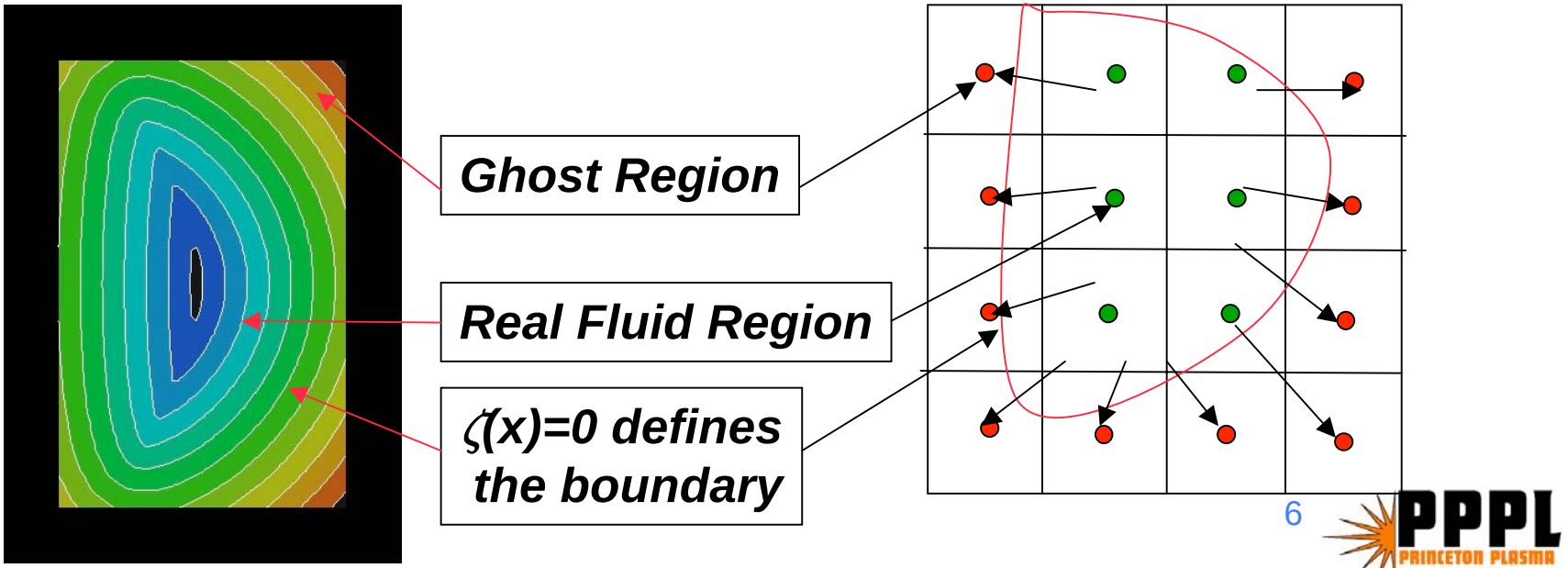

PPPL PRINCETON PLASMA PHYSICS LABORATORY

Level-Set Applied to MHD

- Single fluid resistive MHD equations in conservation form

$$\frac{\partial U}{\partial t}+\frac{1}{R}\frac{\partial RF}{\partial R}+\frac{\partial H}{\partial z}+\frac{1}{R}\frac{\partial G}{\partial \phi}=S+\frac{1}{R}\frac{\partial RF_D}{\partial R}+\frac{\partial H_D}{\partial z}+\frac{1}{R}\frac{\partial G_D}{\partial \phi}+S_D+S_{pellet}$$

Hyperbolic terms ***Diffusive terms***

$$U=\{\rho,\rho u_R,\rho u_\phi,\rho u_Z,B_R,B_\phi,B_Z,e\}^T$$

Density: Ablation
Energy :Electron heat flux

$$F\equiv F(U)=\begin{Bmatrix}\rho u_R\\ \rho u_R^2+p_t-B_R^2\\ \rho u_R u_\phi-B_R B_\phi\\ \rho u_R u_Z-B_R B_Z\\ 0\\ u_R B_Z-u_Z B_R\\ u_R B_\phi-u_\phi B_R\\ (e+p_t)u_R-(B_k u_k)B_R\end{Bmatrix},\quad H\equiv H(U)=\begin{Bmatrix}\rho u_Z\\ \rho u_R u_Z-B_R B_Z\\ \rho u_Z u_\phi-B_Z B_\phi\\ \rho u_Z^2+p_t-B_Z^2\\ u_Z B_R-u_R B_Z\\ 0\\ u_Z B_\phi-u_\phi B_Z\\ (e+p_t)u_Z-(B_k u_k)B_Z\end{Bmatrix},$$

$$G\equiv G(U)=\begin{Bmatrix}\rho u_\phi\\ \rho u_R u_\phi-B_R B_\phi\\ \rho u_\phi^2+p_t-B_\phi^2\\ \rho u_Z u_\phi-B_Z B_\phi\\ u_\phi B_R-u_R B_\phi\\ u_\phi B_Z-u_Z B_\phi\\ 0\\ (e+p_t)u_\phi-(B_k u_k)B_\phi\end{Bmatrix},\quad S(U)=-\frac{1}{R}\begin{Bmatrix}0\\ B_\phi^2-\rho u_\phi^2-p_t\\ \rho u_R u_\phi-B_R B_\phi\\ 0\\ 0\\ 0\\ 0\\ u_\phi B_R-u_R B_\phi\end{Bmatrix}$$

- Semi-analytical Model by Ishizaki et al. (Phys. Plasmas 2000)
  - *–Assumes Maxwellian electrons and neglects pitch angle scattering*
  - *–Requires integrals of density along field lines*
  - *–Challenging to evaluate efficiently for hierarchical meshes (Samtaney et al., SciDAC 2007)*

- Additional constraint $\nabla\cdot\mathbf{B}=0$. Numerically treated with a nonconservative source term $\propto\nabla\cdot B$ (Powell et al 1999)

PPPL PRINCETON PLASMA PHYSICS LABORATORY

Level-set Implementation Details

- Define the fixed plasma boundary Γ(x)
- Compute a *signed* distance function ζ(x) such that
  ζ(x)<0 (>0) denotes the real fluid (ghost fluid) domain
  ζ(x)=0 defines Γ(x)
- Extrapolate quantity q(x,t) from real to ghost region
  - *Constant extrapolation requires* ***n***$\cdot \nabla q = 0$ *where* ***n = n(x)*** *is the normal to the level set function* ζ*(x) defined as* ***n*** $= \nabla \zeta / |\nabla \zeta|$

$$\frac{\partial q}{\partial \tau} + H(\zeta)\mathbf{n} \cdot \nabla q = 0$$

  - *H(*ζ*) is the Heaviside function. The above equation is a linear hyperbolic PDE with characteristics along the direction* ***n****. It reaches steady state a distance x away from the boundary at time=x (because the characteristic speed is unity). At steady state q is extrapolated from the real fluid to the ghost region.*
  - *The above equation is marched forward in time using a first order forward Euler and a first order upwind method (upwind in* ***n****). For linear and quadratic extrapolation consult Aslam (JCP 2003)*
  - *Extrapolate two thermodynamic quantities (density, pressure) and tangential components of the velocity and magnetic fields*
  - *Reflect the normal velocity and magnetic field components to obtain the zero normal flow and perfectly conducting boundary conditions*
- The ghost region 0<ζ(x)<3 Δ x need be filled in for second order method at each stage of the time integration scheme. Once the boundary conditions are set in the ghost region the finite volume inside the real fluid region are updated in the usual fashion

Axisymmetric Localized High-Density Region

- 2D Axisymmetric simulations of the motion of an initially localized high-density high-β region
- Mesh details
  - *Base mesh: 64x64*
  - *2 levels with refinement ratio of 4*
  - *Effective resolution 1024x1024*

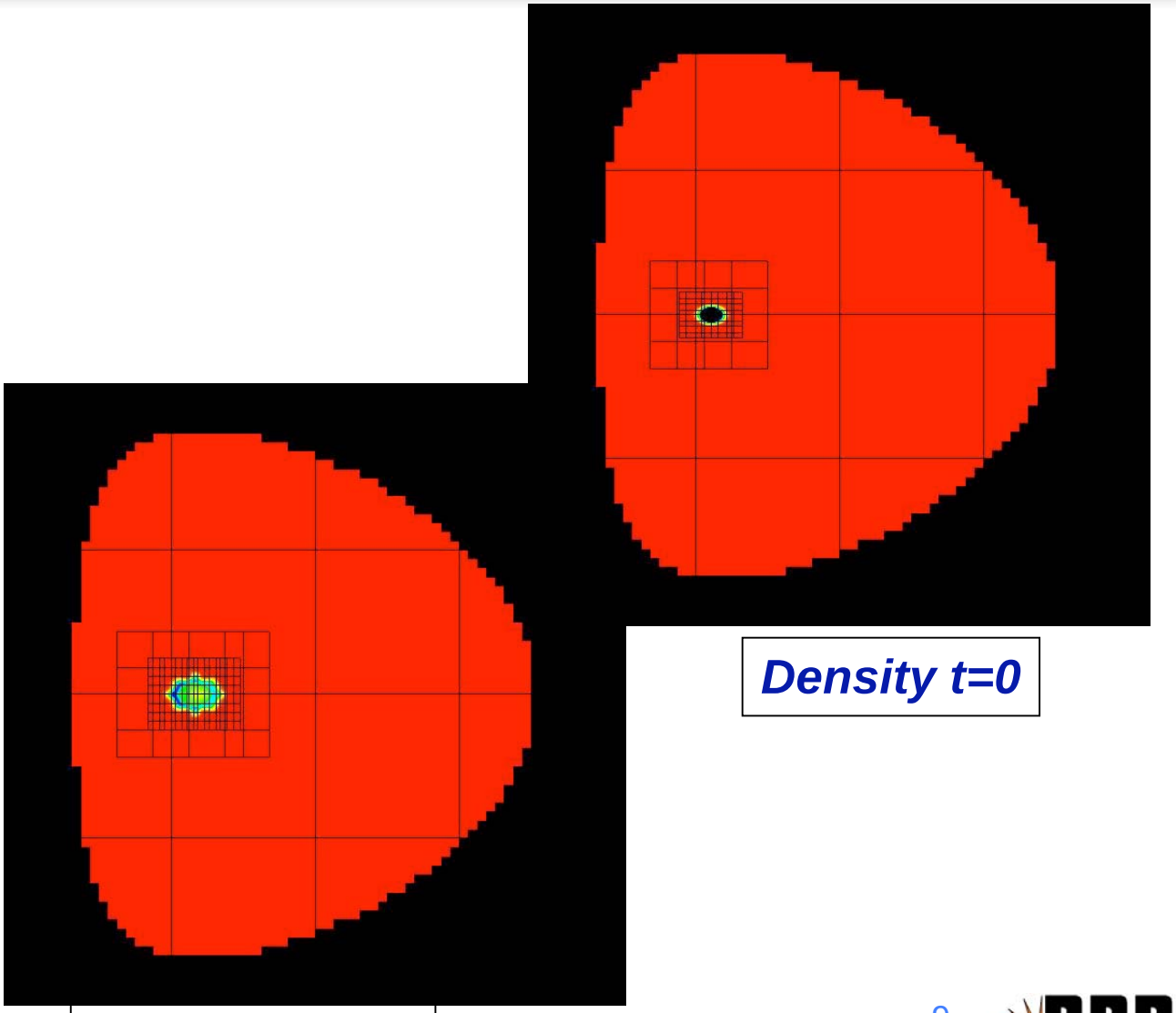

Density t=0

Density t=1.25

PPPL PRINCETON PLASMA PHYSICS LABORATORY

Axisymmetric Localized High-Density Region

- A local minimum in B_ϕ is created on fast time scales. Conditions for an interchange instability are established and the high density blob rapidly translates in the direction of increasing major radius
- The high density region expands, collapses on itself, and propels forward

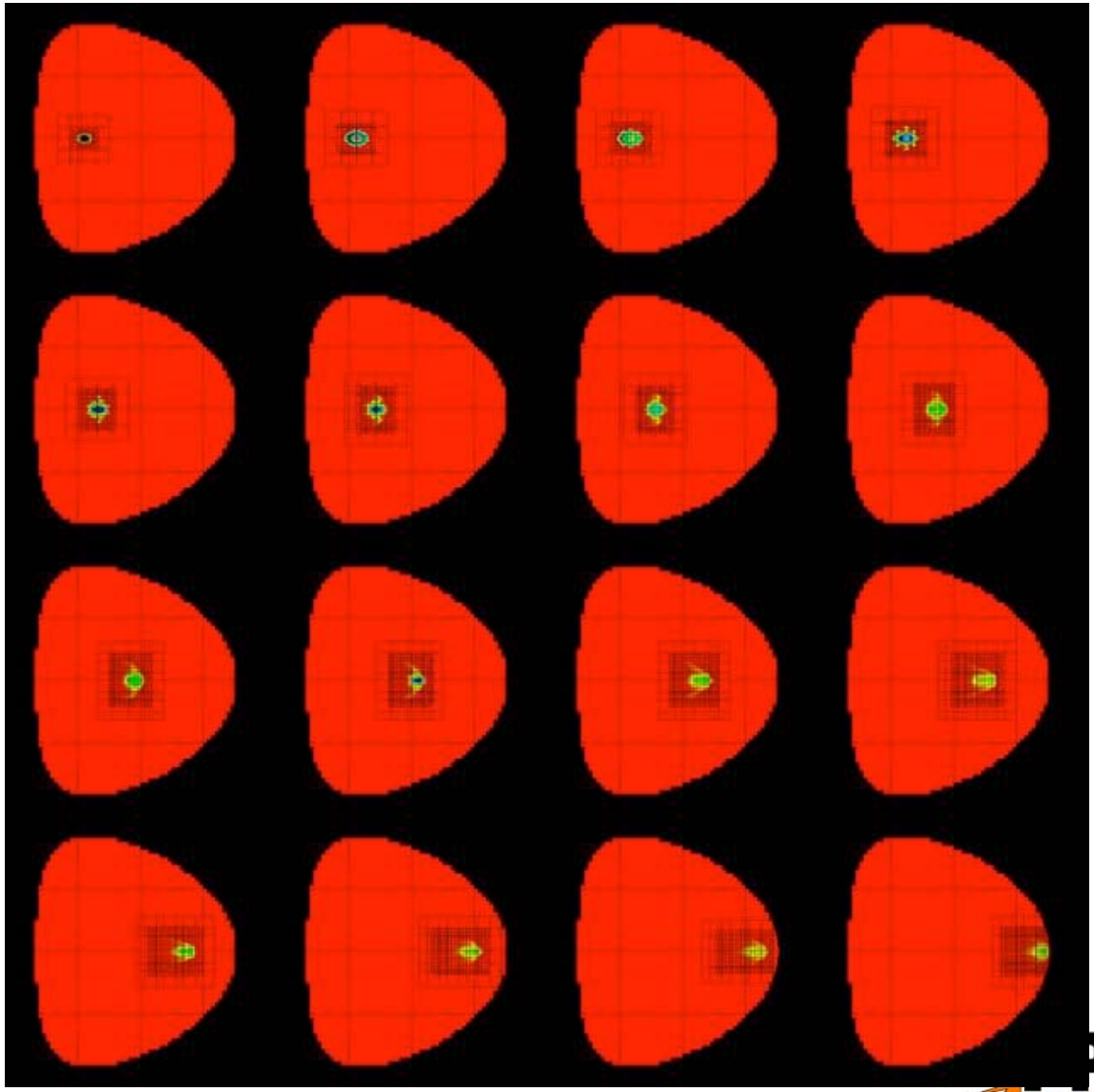

PPPL
PRINCETON PLASMA PHYSICS LABORATORY

Error Estimates and Accuracy

- Motion of an initially smooth Gaussian blob
- Error estimated by computing an "exact" solution at resolution 256 x 256

Variable	L_∞ (64^2)	L_∞ (128^2)	p_∞	L_2 (64^2)	L_2 (128^2)	p_2
Density	0.51e-0	0.13e-0	1.97	4.8e-2	1.07e-2	2.17
U_R	5.08e-5	2.68e-5	0.92	1.15e-5	3.63e-6	1.66
U_Z	7.30e-5	1.81e-5	2.01	1.04e-5	2.94e-6	1.82
U_ϕ	1.53e-6	4.46e-7	1.78	2.0e-7	4.65e-8	2.10
B_R	1.46e-4	1.30e-5	3.49	9.35e-6	5.73e-7	4.02
B_Z	1.17e-4	2.31e-5	2.34	1.02e-5	1.04e-6	3.29
B_ϕ	4.00e-4	1.60e-4	1.32	4.19e-5	1.18e-5	1.83
Pressure	4.11e-4	1.36e-4	1.59	4.23e-5	9.72e-6	2.12

Mass and Energy Conservation

- The boundary representation is implicit and hence mass and energy are not conserved to machine accuracy

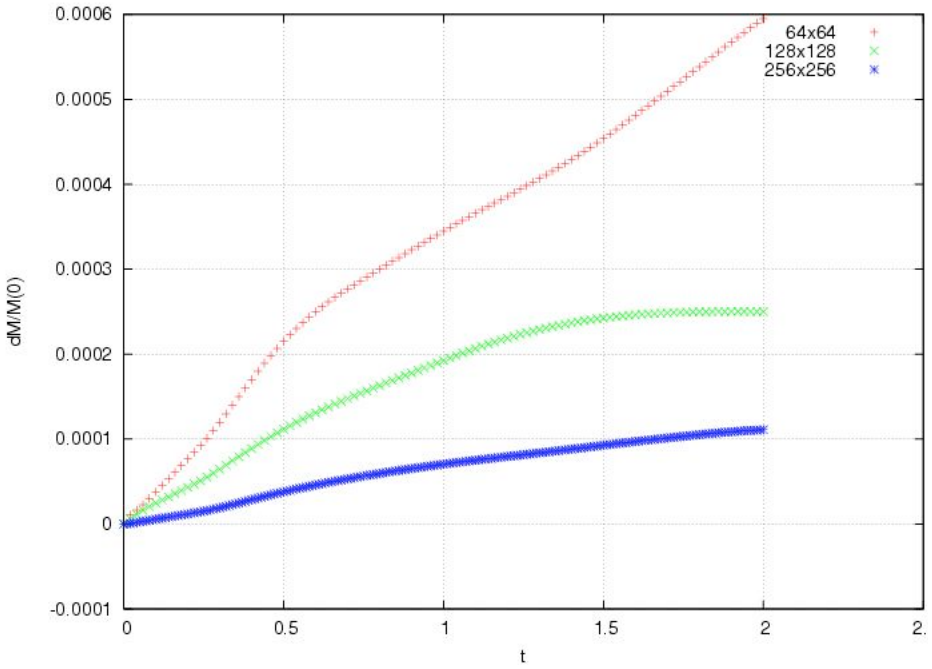

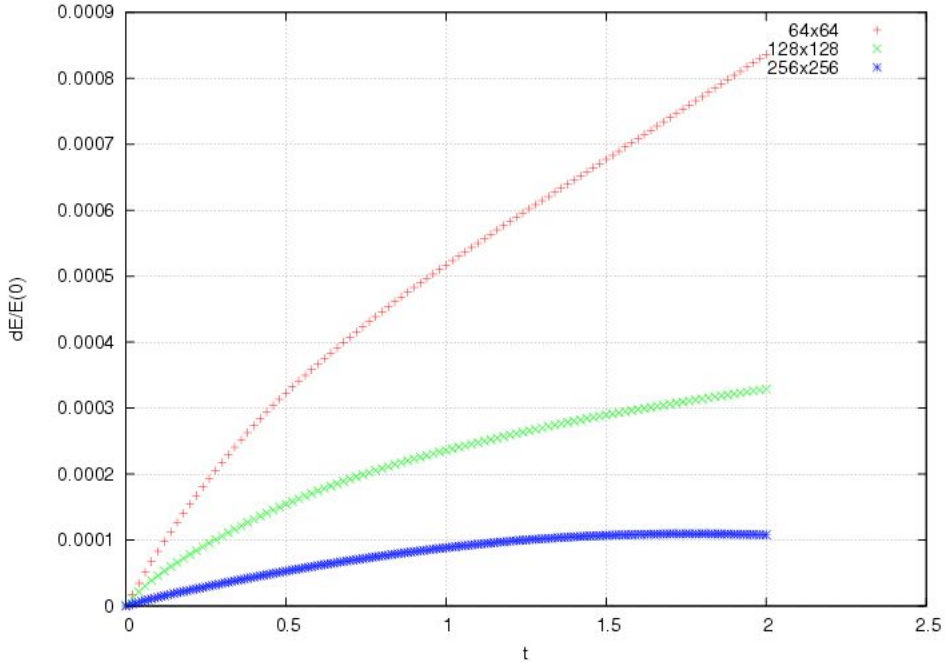

PPPL PRINCETON PLASMA PHYSICS LABORATORY

3D Localized High-Density Region

- 3D simulations of the motion of an initially localized high-density high-β region
- Details
  - *$\phi \in [-\pi/16, \pi/16]$*
  - *Tokamak geometry*
  - *Visualization in computational space*
  - *Base mesh: 64x64x64*
  - *1 level with refinement ratio of 4*
  - *Effective resolution 256x256x256*
  - *2 level run on Cray XT4 at NERSC still to be diagnosed due to the size of the data sets (~500-650 Mb/ time step)*

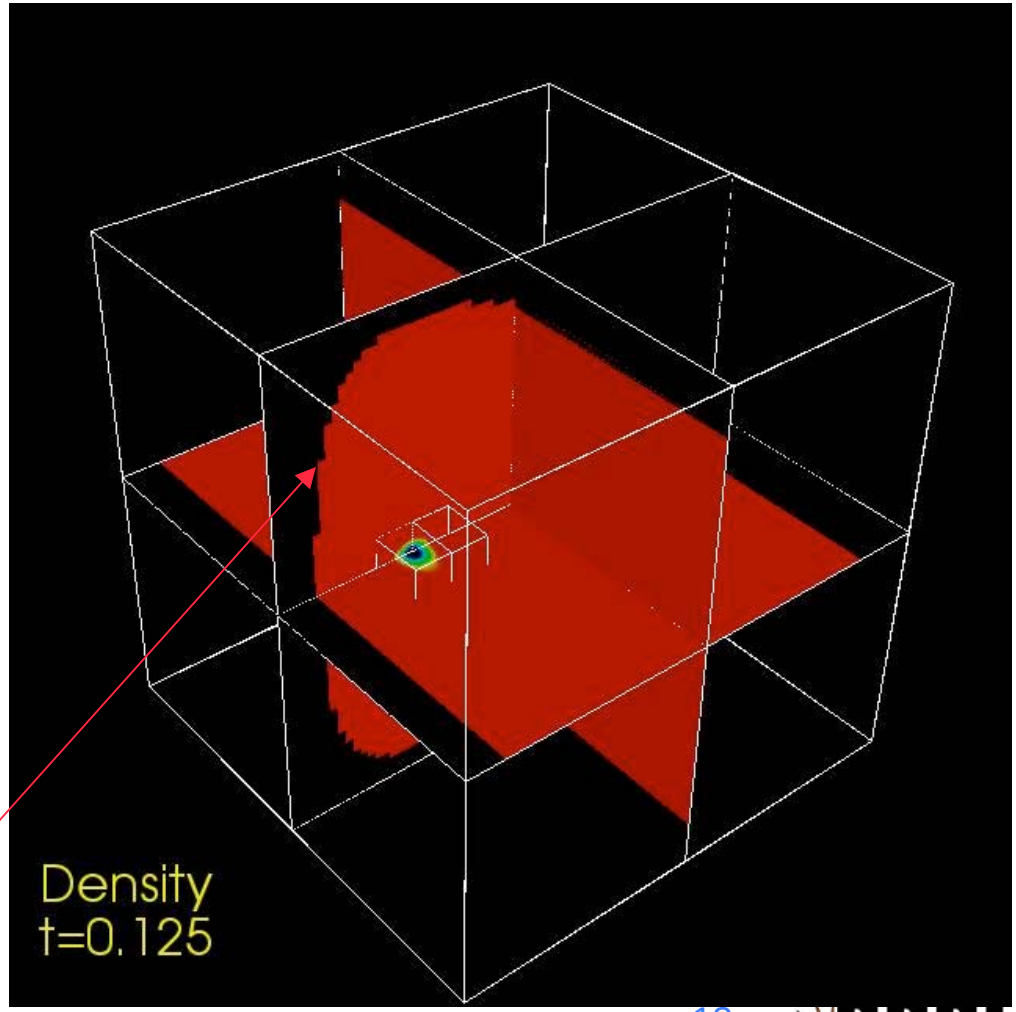

Note: Staircasing is a visualization feature; the actual boundary is smooth

PPPL PRINCETON PLASMA PHYSICS LABORATORY

3D Localized High-Density Region

- Dominant flow in toroidal direction
- High density region is short-lived
- Maximum density
  - *t=0* ρ_{max}*=1000*
  - *t=0.125* ρ_{max}*=150*
  - *t=0.625* ρ_{max}*=60*
  - *t=1.25* ρ_{max}*=10*
  - *t=3.75* ρ_{max}*=2.2*
  - *t=6.25* ρ_{max}*=1.15*

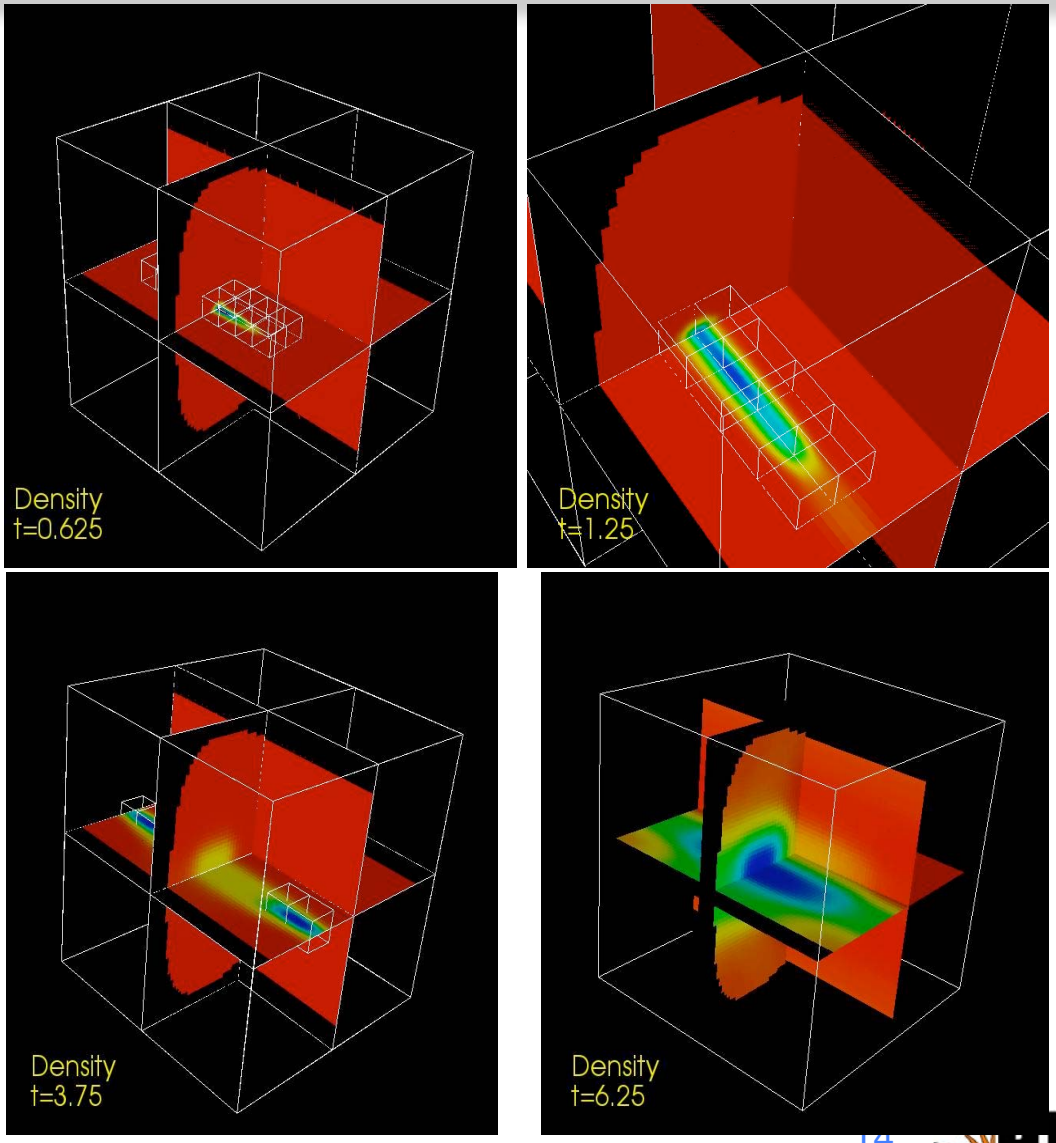

PPPL PRINCETON PLASMA PHYSICS LABORATORY

3D Localized High-Density Region

- Local minimum in B_ϕ at early times
- B_ϕ recovers its initial equilibrium value by t=1.25

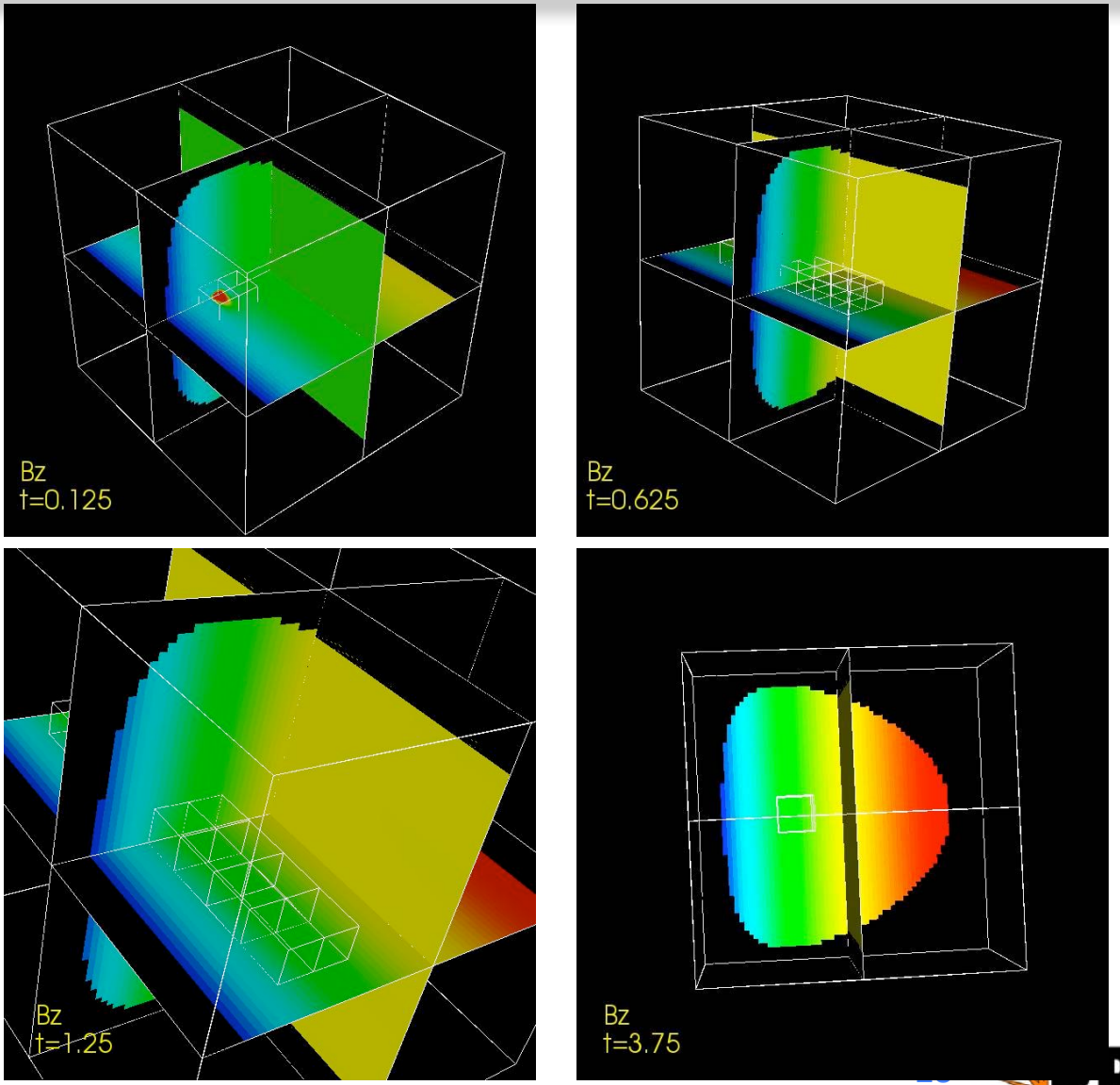

PPPL PRINCETON PLASMA PHYSICS LABORATORY

3D Localized High-Density Region

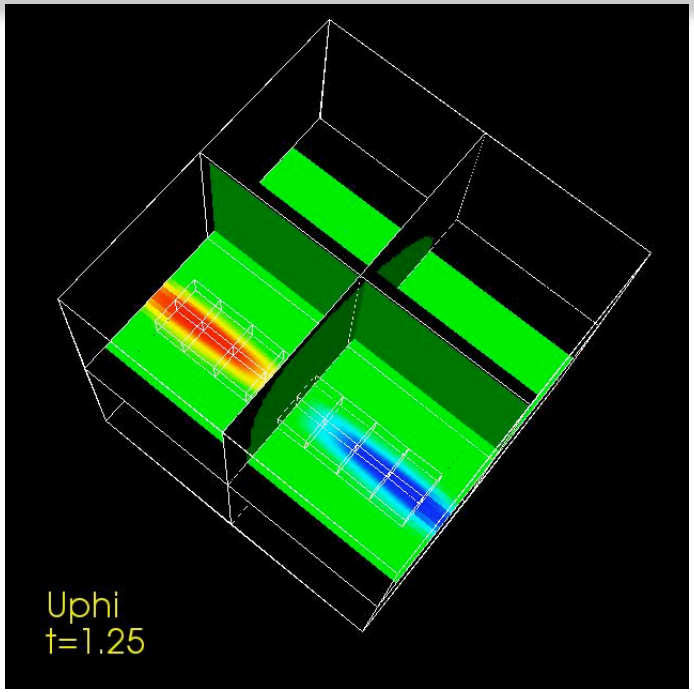

U_ϕ range (-0.13,0.13)

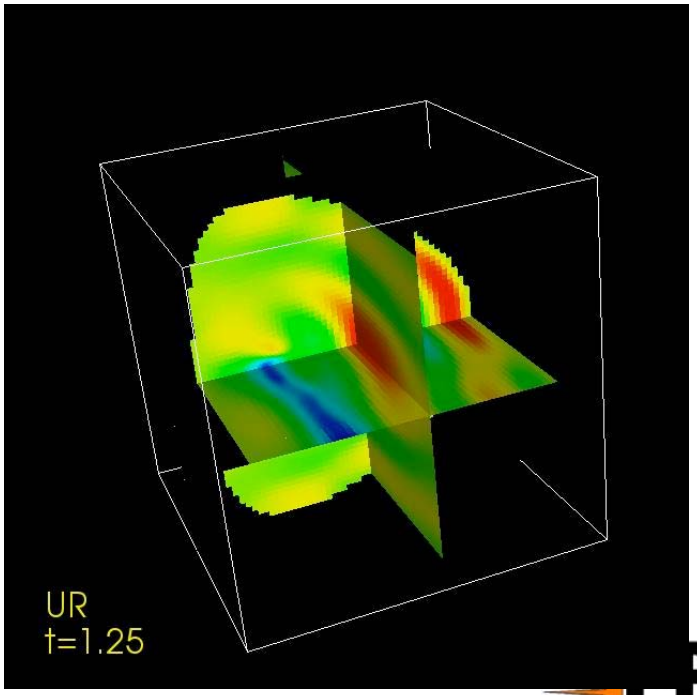

U_R range (-0.007,0.014)

PPPL
PRINCETON PLASMA PHYSICS LABORATORY

3D Localized High-Density Region

- Pressure

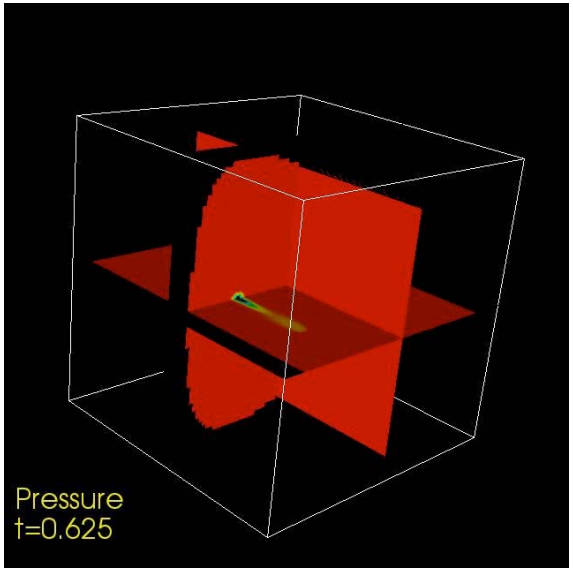

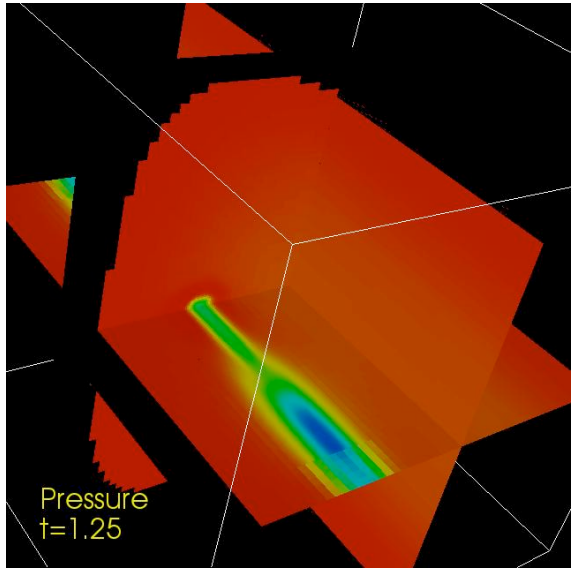

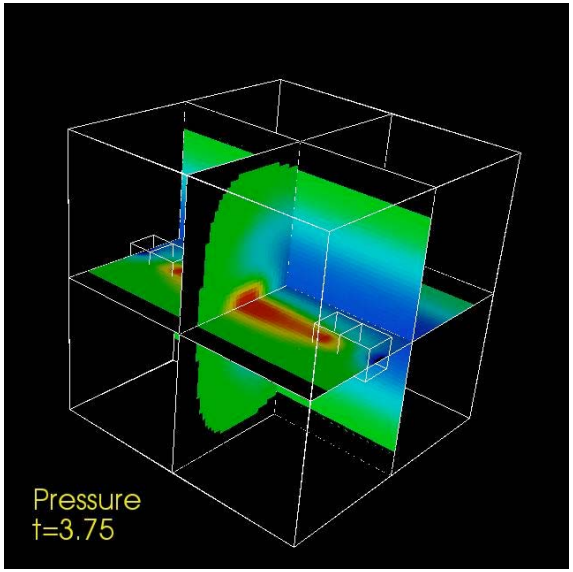

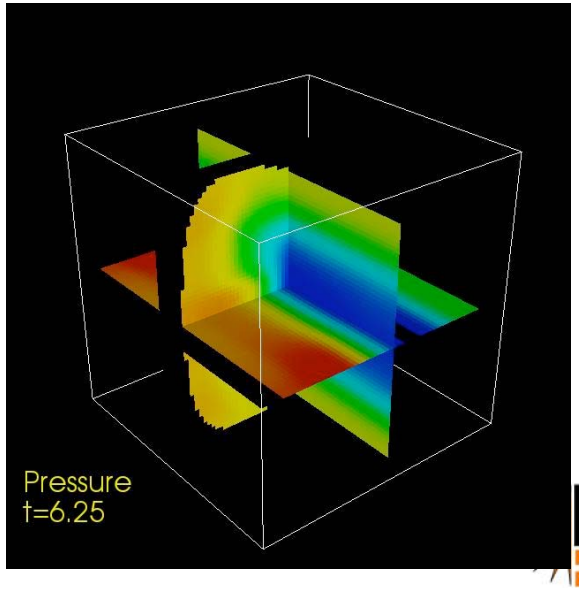

PPPL
PRINCETON PLASMA PHYSICS LABORATORY

Electron Heat Flux Model

- Semi-analytical Model by Parks et al. (Phys. Plasmas 2000)
  - *Assumes Maxwellian electrons and neglects pitch angle scattering*

$$-\nabla \cdot q_e = \frac{q_\infty n}{\tau_\infty}\left[g(u_+) + g(u_-)\right]$$

Where $g(u) = u^{\frac{1}{2}} K_1(u^{\frac{1}{2}})/4$, $u_\pm = \frac{\tau_\pm}{\tau_\infty}$ *and* $\tau_\pm = \pm \int_{\mp\infty}^{x} n(s)ds$

K_1 is modified Bessel function of the second kind, and

$$q_\infty = \sqrt{\frac{2}{\pi m_e}} n_{e\infty} (k\, T_{e\infty})^{\frac{3}{2}} \qquad \tau_\infty = \frac{T_{e\infty}^2}{8\pi e^4 \log\Omega}$$

- Energy is not conserved because the electron heating model acts as an energy source with no corresponding energy sink along field lines to balance it

AMR Opacity Computation

- Grid refinement strategy ensures that the pellet cloud is completely contained within the finest level. Set τ=0 in ghost cells. Assume ρ_{amb}<<ρ

$$\int_{-\infty}^{0}(\rho-\rho_{amb})ds = \int_{\kappa}^{0}(\rho-\rho_{amb})ds + \int_{-\infty}^{\kappa}(\rho-\rho_{amb})ds$$
$$\int_{-\infty}^{0}(\rho-\rho_{amb})ds \approx \int_{\kappa}^{0}(\rho-\rho_{amb})ds + 0$$

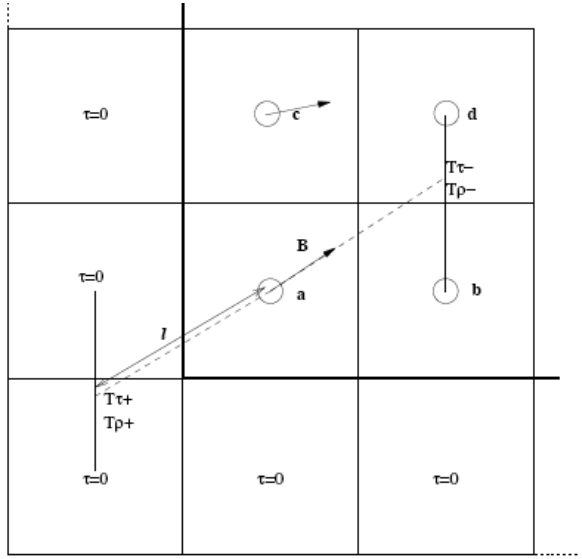

- The upstream values of ρ and τ are computed using linear interpolation
  - *The value of τ is initialized on the grid boundary.*

$$\int_{\kappa}^{a}\rho ds \approx \int_{\kappa}^{T}\rho ds + \int_{T}^{a}\rho ds, \quad = \tau_T + l\frac{\rho_T+\rho_a}{2}$$

- This computation is iterated until convergence. Points get updated in a traveling wave for each τ_+ and τ_- (In the figure points a & c have τ_+ updated first)
- In a parallel multiblock AMR calculation each box first performs integration of τ with values filled into its ghost cells from neighboring boxes. The box-by-box integration is repeated until convergence.

PPPL PRINCETON PLASMA PHYSICS LABORATORY

HFS Pellet Injection Simulation

- Grid statistics
  - *Base mesh: 64 x 64 x 64*
  - *4 levels of refinement with a factor of 2*
  - *Equivalent fine mesh: 1024^3*
  - *Finest mesh volume~ 0.00027 x total volume*
- Domain is a one-eighth sector of a tokamak
- Pellet radius = 1mm
- Toroidal field on axis = 1T
- “Far away” electron temperature = 4Kev
- Parks heating model
  - *Ablation determined by computing computing the incident heat flux on the pellet surface*
    - *All the incident heat flux goes to sublimate the pellet*
    - *Overestimates ablation at early times (because dissociation and ionization are neglected)*

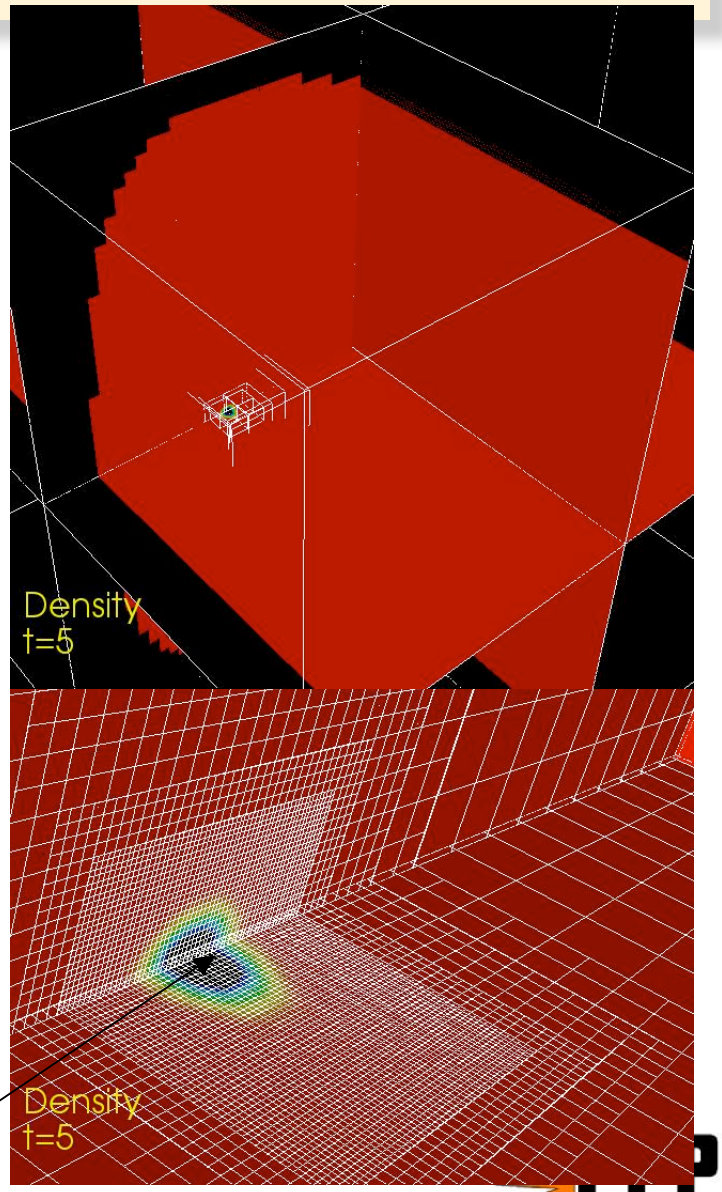

ρ_{max}~2 x 10^6

PRINCETON PLASMA PHYSICS LABORATORY

HFS Pellet Injection Simulation

- By t=5, the electron heat flux increases the pressure increases to 0.1 (local β = 0.35)
  - *This is insufficient to trigger the rapid instability seen in the earlier 3D simulation of the localized high-density high-β region*
  - *There is no local minimum yet in B_ϕ*
- The high pressure region is a 3D annulus around the pellet caused by the electron heat flux

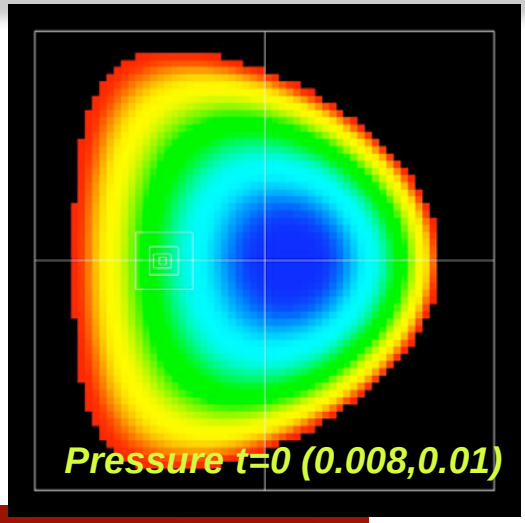

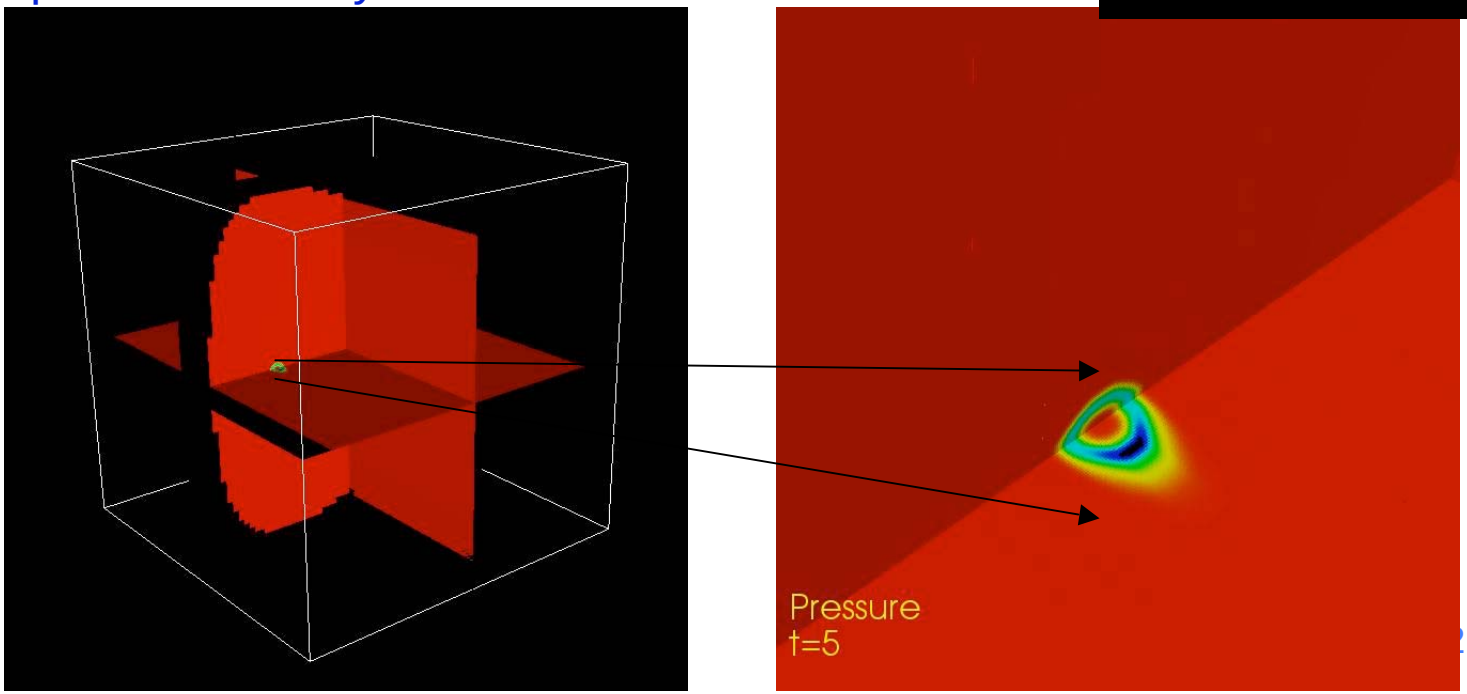

PPPL PRINCETON PLASMA PHYSICS LABORATORY

HFS Pellet Injection Simulation

- The toroidal magnetic field is not very different from the initial condition
- The pellet ablated material flows along field lines in the toroidal direction

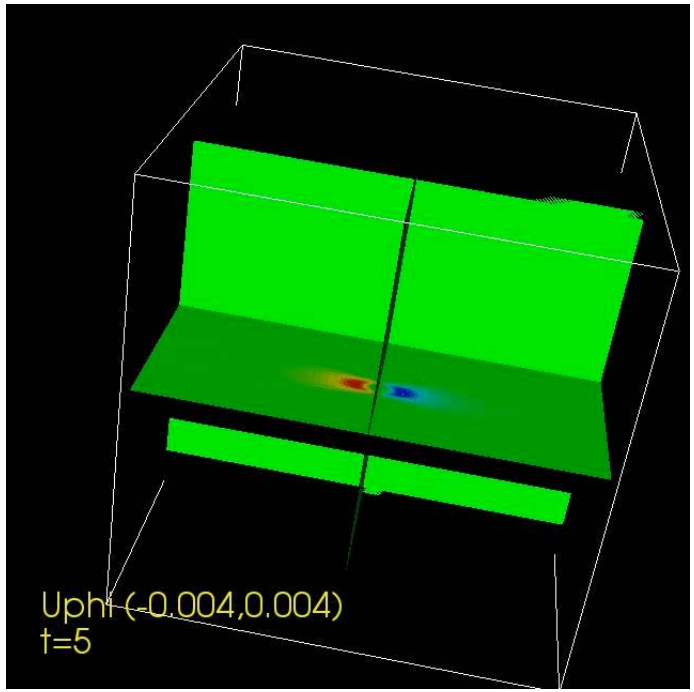

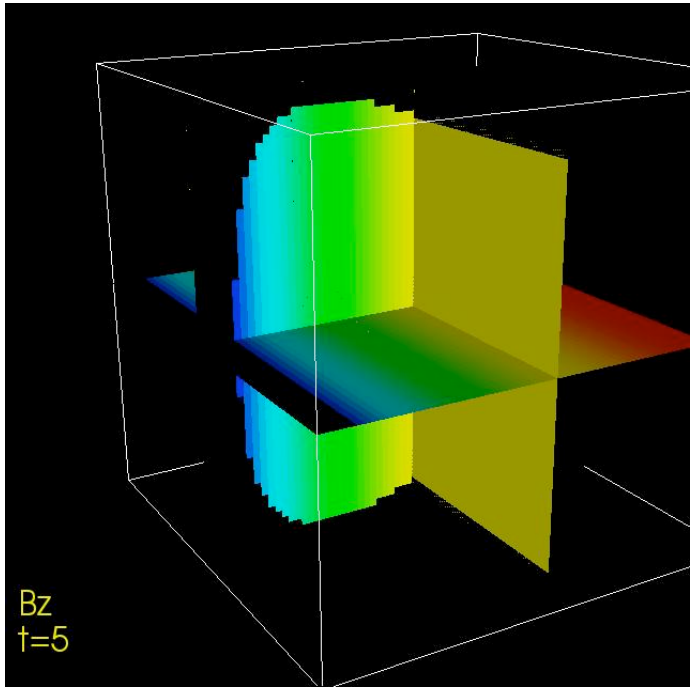

PPPL PRINCETON PLASMA PHYSICS LABORATORY

JFNK Method for Resistive MHD

- Resistive MHD written in conservation form

$$\partial_t \rho + \nabla \cdot (\rho \mathbf{v}) = 0,$$
$$\partial_t (\rho \mathbf{v}) + \nabla \cdot \left(\rho \mathbf{v}\mathbf{v}^T - \mathbf{B}\mathbf{B}^T + (p + \tfrac{1}{2}\mathbf{B}\cdot\mathbf{B})\,\bar{\mathrm{I}} \right) = \nabla \cdot \bar{\tau},$$
$$\partial_t \mathbf{B} + \nabla \cdot \left(\mathbf{v}\mathbf{B}^T - \mathbf{B}\mathbf{v}^T \right) = \nabla \cdot \left(\eta \nabla \mathbf{B} - \eta\,(\nabla \mathbf{B})^T \right),$$
$$\partial_t e + \nabla \cdot \left((e + p + \tfrac{1}{2}\mathbf{B}\cdot\mathbf{B})\mathbf{v} - \mathbf{B}(\mathbf{B}\cdot\mathbf{v}) \right) = \nabla \cdot (\bar{\tau}\mathbf{v} + \kappa \nabla T) + \nabla \cdot \left(\eta \left(\tfrac{1}{2}\nabla(\mathbf{B}\cdot\mathbf{B}) - \mathbf{B}(\nabla \mathbf{B})^T \right) \right)$$

- Rewriting

$$\mathbf{U} = (\rho,\ \rho\mathbf{v},\ \mathbf{B},\ e)^T$$

$$\partial_t \mathbf{U} = -\nabla \cdot \mathbf{F}_h(\mathbf{U}) + \nabla \cdot \mathbf{F}_v(\mathbf{U}) = \nabla \cdot \mathbf{F}(\mathbf{U}).$$

- The solution at the next time level to the entire system of equations is expressed as the solution to the following nonlinear equation

$$\mathcal{F}(U^{n+1}) = U^{n+1} - U^n + (1-\theta)R(U^{n+1}) + \theta R(U^n) = 0$$

- This is solved using Newton's method (For an alternative approach with nonlinear multigrid for MHD, please visit the poster by Adams & Samtaney, Poster 12 Session 1B, Monday)

$$\delta U^k = -\left[\left(\frac{\partial \mathcal{F}}{\partial U} \right)^{n+1,k} \right]^{-1} \mathcal{F}$$

where $J(U^{n+1,k}) \equiv \left(\frac{\partial \mathcal{F}}{\partial U}\right)^{n+1,k}$ is the Jacobian; and $\delta U^k \equiv U^{n+1,k+1} - U^{n+1,k}$

JFNK: Solvers and Preconditoners

- The linear system at each Newton iteration is solved with a Krylov method in which an approximation to the linear system J $\delta U = -\mathcal{F}$ is obtained by iteratively building a Krylov subspace of dimension m

$$\mathcal{K}(r_0, J) = span\{r_0, Jr_0, J^2 r_0, \cdots, J^{m-1} r_0\}$$

- Krylov methods can lead to slow convergence. This is especially true for MHD where the Jacobian is ill-conditioned. Preconditioners help alleviate the problem of slow convergence and are formulated as follows

$$\begin{aligned}
(J(U^k)P^{-1})(P\delta U^k) &= -\mathcal{F}(U^{n+1,k}) \quad (Right), \\
(P^{-1}J(U^k))\delta U^k &= -P^{-1}\mathcal{F}(U^{n+1,k}) \quad (Left), \\
(P_L^{-1}J(U^k)P_R^{-1})(P_R\delta U^k) &= -P_L^{-1}\mathcal{F}(U^{n+1,k}) \quad (Both).
\end{aligned}$$

- The basic idea of preconditioners is that the matrix JP^{-1} or $P^{-1}J$ is close to the identity matrix, i.e., P is a good approximation of J. Furthermore, to make preconditioning effective, P^{-1} should be computationally inexpensive to evaluate

JFNK: Resistive MHD - Preconditioner

- Instead of solving J δ U = -g solve (J P^{-1}) (P δ U) = -g, i.e., right preconditioning is employed
- The preconditioner takes into account the local wave structure
  - *Preconditioner is exact for any 1D system of hyperbolic conservation laws*
- The preconditioner is split into a hyperbolic and a diffusive component

$$P^{-1} = P_h^{-1} P_d^{-1} = J(\mathbf{U})^{-1} + \mathcal{O}(\Delta t^2)$$

- Denoting by (.) the location of the linear operator action, the ideal MHD Jacobian is

$$\begin{aligned} J_h(\mathbf{U}) &= I + \overline{\gamma}\left[J_x \partial_x(\cdot) + J_y \partial_y(\cdot) + J_z \partial_z(\cdot)\right] \\ &= I + \overline{\gamma}\left[J_x L_x^{-1} L_x \partial_x(\cdot) + J_y L_y^{-1} L_y \partial_y(\cdot) + J_z L_z^{-1} L_z \partial_z(\cdot)\right] \\ &= I + \overline{\gamma}\left[J_x L_x^{-1} \partial_x\left(L_x(\cdot)\right) - J_x L_x^{-1} \partial_x(L_x)(\cdot)\right. \\ &\quad + J_y L_y^{-1} \partial_y\left(L_y(\cdot)\right) - J_y L_y^{-1} \partial_y(L_y)(\cdot) \\ &\quad \left. + J_z L_z^{-1} \partial_z\left(L_z(\cdot)\right) - J_z L_z^{-1} \partial_z(L_z)(\cdot)\right] \end{aligned}$$

where J_x is the Jacboian of the hyperbolic flux in the x-direction. L_x is the spatially local left eigenvector matrix for J_x. J_y, L_y, J_z, and L_z are similarly defined

JFNK: Resistive MHD - Preconditioner

- Directional splitting is employed to further approximate the preconditioner

$$
\begin{aligned}
P_h = & \left[I + \overline{\gamma} J_x L_x^{-1} \partial_x (L_x(\cdot))\right] \left[I + \overline{\gamma} J_y L_y^{-1} \partial_y (L_y(\cdot))\right] \left[I + \overline{\gamma} J_z L_z^{-1} \partial_z (L_z(\cdot))\right] \\
& \left[I - \overline{\gamma} \left(J_x L_x^{-1} \partial_x \left(L_x\right) + J_y L_y^{-1} \partial_y \left(L_y\right) + J_z L_z^{-1} \partial_z \left(L_z\right)\right)\right] \\
= & \, P_x \, P_y \, P_z \, P_{\text{corr}}.
\end{aligned}
$$

- Decoupling into 1D wave equations along characteristics

$$
\begin{aligned}
& L_i(x) J_i(x) = \Lambda_i(x) L_i(x), \quad \Lambda_i = \mathrm{Diag}(\lambda^1, \ldots, \lambda^8) \\
& L_i \left[I + \overline{\gamma} J_i L_i^{-1} \partial_i (L_i(\cdot))\right] \xi = L_i \beta \quad \Leftrightarrow \quad \zeta + \overline{\gamma} \, \Lambda_i \, \partial_i \zeta = \chi,
\end{aligned}
$$

where $\zeta = L_i \xi$ and $\chi = L_i \beta$

- Thus along each direction, we get a system of linear wave equations. For each wave family, we now get a sequence of tridiagonal linear systems which can be efficiently solved. In parallel we use the method proposed by Arbenz & Gander (1994)

JFNK: Resistive MHD - Preconditioner

- For spatially varying J(U) a correction solve is involved

$$P_{\text{corr}} = I - \overline{\gamma}\left[J_x L_x^{-1}\partial_x\left(L_x\right) + J_y L_y^{-1}\partial_y\left(L_y\right) + J_z L_z^{-1}\partial_z\left(L_z\right)\right]$$
$$= I - \overline{\gamma}\left[L_x^{-1}\Lambda_x\partial_x\left(L_x\right) + L_y^{-1}\Lambda_y\partial_y\left(L_y\right) + L_z^{-1}\Lambda_z\partial_z\left(L_z\right)\right]$$

- Since this has no spatial couplings, the resulting local block systems may be solved easily by precomputing the 8x8 block matrices P_{corr} at each location coupled with a LU factorization
- Only the fastest stiffness inducing waves need to be solved. Furthermore, accuracy may be sacrificed because this is done in the context of the preconditioner.
- It can be shown that the error bound (Reynolds, Samtaney, Woodward, 2008) if q-fastest waves are preconditioned is

$$\left\|\chi - \hat{\chi}\right\|_p \leq \left\|L_F^{-1}\right\|_p \left[\sum_{l=q+1}^{n}\left(\frac{\left\|\Delta t\lambda^l\partial_x(\cdot)\right\|_p}{1-\left\|\Delta t\lambda^l\partial_x(\cdot)\right\|_p}\right)^p \left\|\left(L_F b\right)^l\right\|_p^p\right]^{1/p}$$

- Error from preconditioning q-fastest waves is dominantly $\dfrac{\left|\Delta t\lambda^{q+1}/\Delta x\right|}{1-\left|\Delta t\lambda^{q+1}/\Delta x\right|}$
  - *Omission of waves with small speeds compared to the dynamical time scale will not significantly affect the precondtioner accuracy*

JFNK: Resistive MHD - Preconditioner

- Diffusion Preconditioner P_d: This solves the subsystem $\partial_t \mathbf{U} - \nabla \cdot \mathbf{F}_v = 0$

$$P_d = J_v(\mathbf{U}) = I - \overline{\gamma}\frac{\partial}{\partial \mathbf{U}}\left(\nabla \cdot \mathbf{F}_v\right)$$

$$= \begin{bmatrix} I & 0 & 0 & 0 \\ 0 & I - \overline{\gamma} D_{\rho\mathbf{v}} & 0 & 0 \\ 0 & 0 & I - \overline{\gamma} D_{\mathbf{B}} & 0 \\ -\overline{\gamma} L_\rho & -\overline{\gamma} L_{\rho\mathbf{v}} & -\overline{\gamma} L_{\mathbf{B}} & I - \overline{\gamma} D_e \end{bmatrix}$$

- To solve $P_d\, y = b$ for $y = [\, y_\rho, y_{\rho\,\mathbf{v}}, y_{\mathbf{B}}, y_e]^T$

1. Update $y_\rho = b_\rho$
2. Solve $\left(I - \overline{\gamma} D_{\rho\mathbf{v}}\right) y_{\rho\mathbf{v}} = b_{\rho\mathbf{v}}$ for $y_{\rho\mathbf{v}}$
3. Solve $\left(I - \overline{\gamma} D_{\mathbf{B}}\right) y_{\mathbf{B}} = b_{\mathbf{B}}$ for $y_{\mathbf{B}}$
4. Update $\tilde{b}_e = b_e + \overline{\gamma}\left(L_\rho\, y_\rho + L_{\rho\mathbf{v}}\, y_{\rho\mathbf{v}} + L_{\mathbf{B}}\, y_{\mathbf{B}}\right)$
5. Solve $\left(I - \overline{\gamma} D_e\right) y_e = \tilde{b}_e$ for y_e.

Steps 2,3 and 5 are solved using a geometric multigrid approach. Step 4 may be approximated with finite differences instead of constructing and multiplying by individual submatrices

$$L_\rho\, y_\rho + L_{\rho\mathbf{v}}\, y_{\rho\mathbf{v}} + L_{\mathbf{B}}\, y_{\mathbf{B}} = \frac{1}{\sigma}\left[\nabla \cdot \mathbf{F}_v(U + \sigma W) - \nabla \cdot \mathbf{F}_v(\mathbf{U})\right]_e + O(\sigma),$$

where $W = [y_\rho, y_{\rho\mathbf{v}}, y_{\mathbf{B}}, 0]^T$

PPPL PRINCETON PLASMA PHYSICS LABORATORY

Verification Tests

Linear wave propagtion test.

Computational time for an explicit method scales as $S^{3/2}$

Initial conditions: Perturbed Harris sheet proposed by Birn et al. (J. Geo. Lett. 2001)

Pellet Model Problem with a similar separation of scale as the tokamak case.

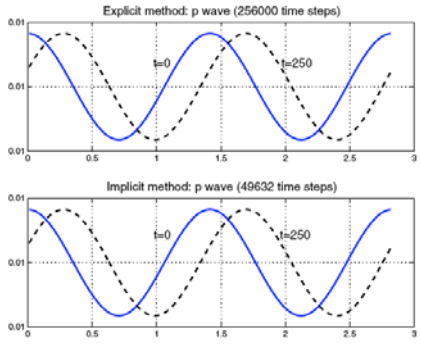

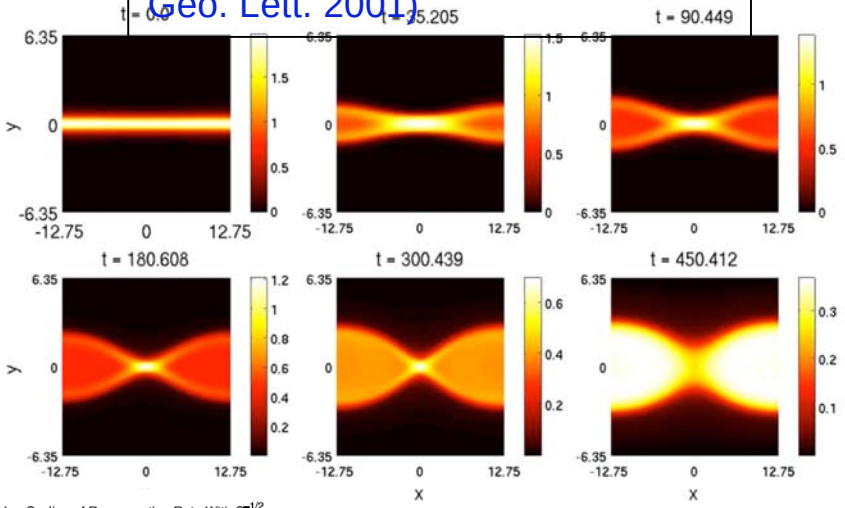

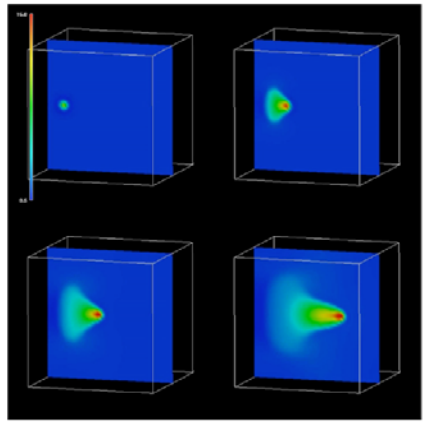

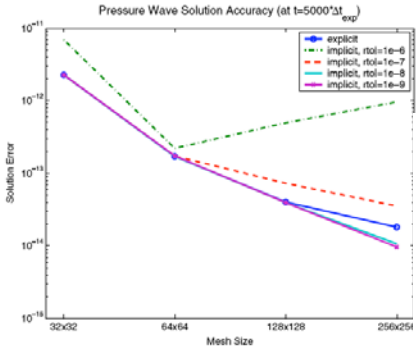

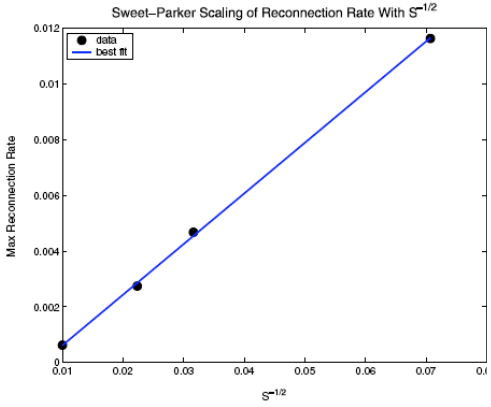

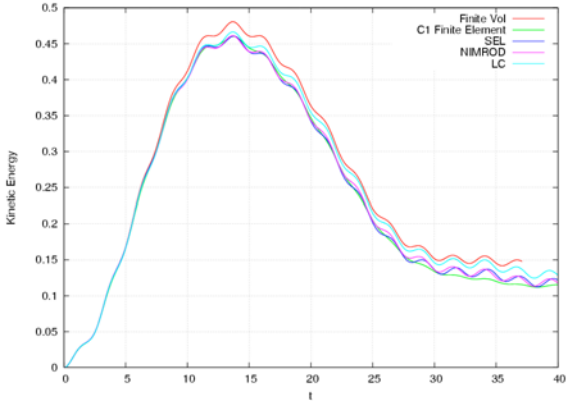

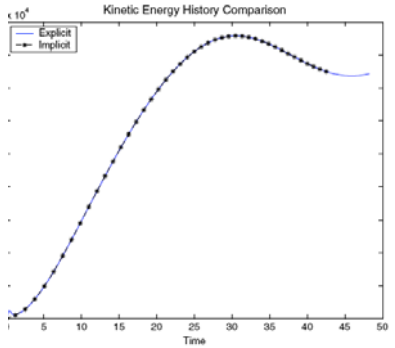

From Reynolds, Samtaney & Woodward, JCP 2006

PPPL PRINCETON PLASMA PHYSICS LABORATORY

Verification Test: Linear Wave Propagation

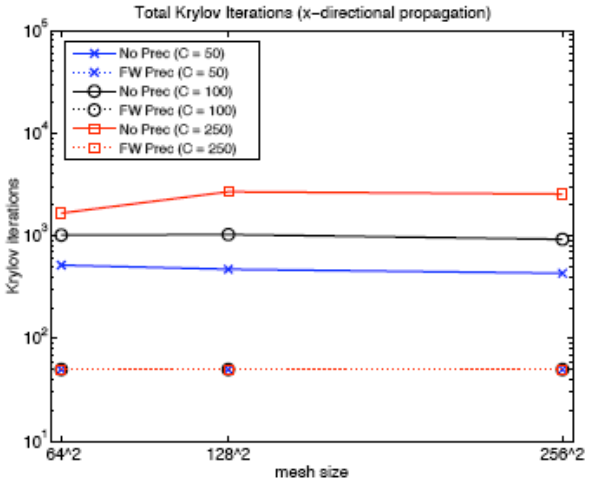

(a) Krylov iterations (x-dir.)

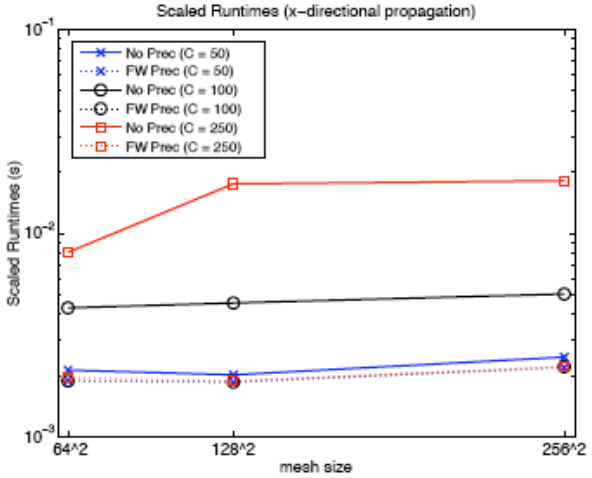

(b) scaled CPU (x-dir.)

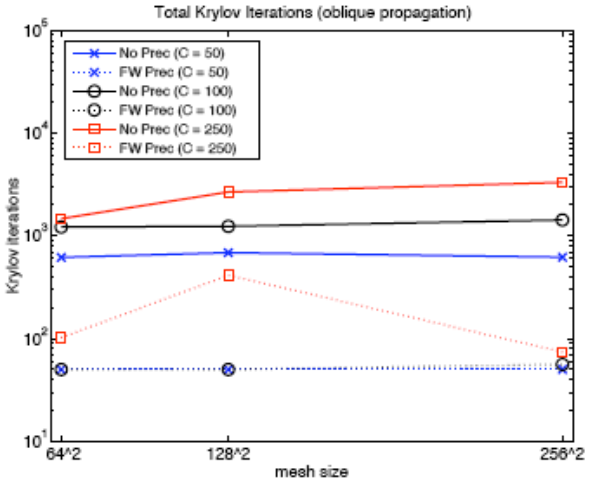

(c) Krylov iterations (oblique)

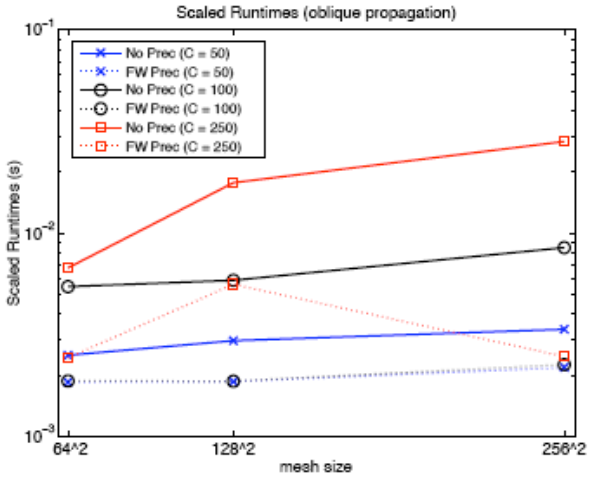

(d) scaled CPU (oblique)

PPPL PRINCETON PLASMA PHYSICS LABORATORY

Verification Test: Kelvin-Helmholtz

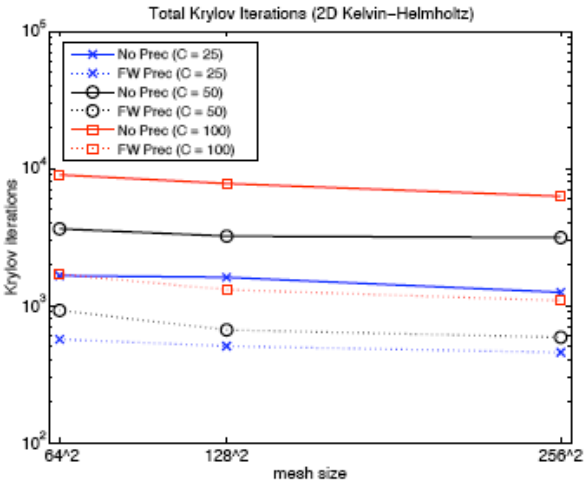

(a) Krylov iterations (2D)

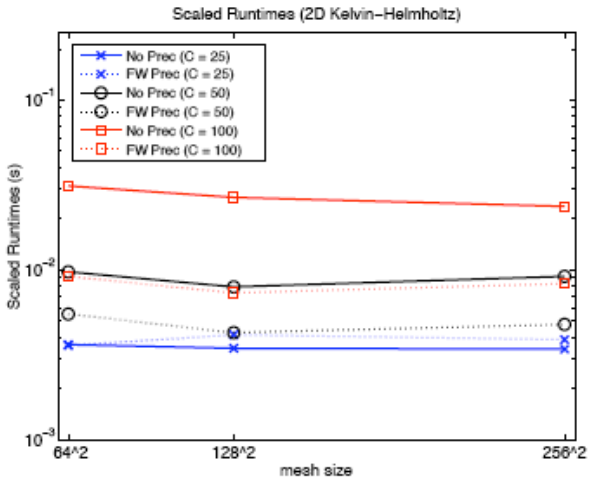

(b) scaled CPU (2D)

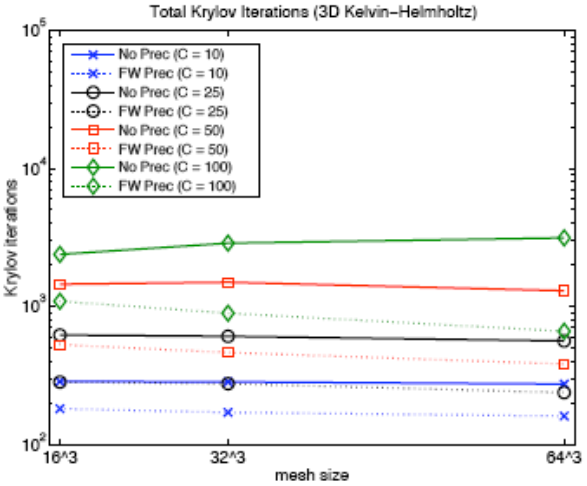

(c) Krylov iterations (3D)

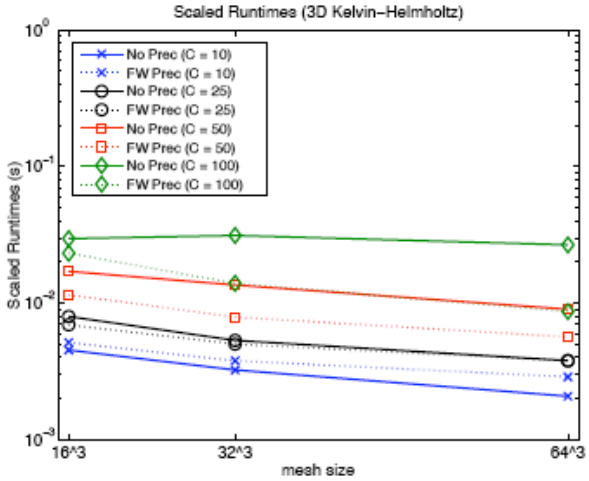

(d) scaled CPU (3D)

PPPL PRINCETON PLASMA PHYSICS LABORATORY

Preconditioner Optimizations

Mesh	Prec	$C = 50$ Krylov	$C = 50$ CPU	$C = 100$ Krylov	$C = 100$ CPU	$C = 250$ Krylov	$C = 250$ CPU
64^2	8	50	7.4	50	7.4	60	7.9
64^2	8 NC	50	5.3	52	5.4	208	10.6
64^2	8 NC-f	50	5.2	52	5.3	208	10.5
64^2	4 NC	50	**4.6**	50	**4.6**	60	**4.9**
64^2	2 NC	50	5.2	50	4.8	60	5.3
128^2	8	52	29.9	50	29.9	50	29.7
128^2	8 NC	50	**20.5**	50	20.9	50	**20.7**
128^2	8 NC-f	50	20.8	50	**20.8**	50	20.8
128^2	4 NC	50	20.7	136	33.0	61	21.3
128^2	2 NC	50	23.7	136	32.2	61	22.2
256^2	8	50	141.1	51	141.9	202	255.9
256^2	8 NC	50	104.2	50	107.5	189	186.0
256^2	8 NC-f	50	105.9	50	105.3	189	185.8
256^2	4 NC	53	**101.4**	50	**98.6**	179	**172.5**
256^2	2 NC	53	102.5	50	107.0	179	187.1
512^2	8	50	655.6	53	635.0	88	**750.2**
512^2	8 NC	50	505.7	52	**485.8**	389	1396
512^2	8 NC-f	50	**505.2**	52	**485.8**	389	1399
512^2	4 NC	68	571.2	158	709.1	389	1273
512^2	2 NC	68	582.7	158	819.3	389	1508

Linear wave test

KH 2D test

Mesh	Prec	$C = 25$ Krylov	$C = 25$ CPU	$C = 50$ Krylov	$C = 50$ CPU	$C = 100$ Krylov	$C = 100$ CPU
128×64	8	791	96.3	1354	142.2	4783	469.9
128×64	8 NC	734	62.7	1367	99.8	3295	240.1
128×64	8 NC-f	694	52.5	1049	**77.6**	2130	**141.8**
128×64	4 NC	735	53.5	1360	91.7	3309	208.0
128×64	2 NC	741	**50.6**	1313	77.9	3255	186.8
256×128	8	679	441.4	1197	562.1	3617	1525
256×128	8 NC	620	297.3	1130	366.2	2809	849.7
256×128	8 NC-f	589	267.0	893	296.2	1497	**436.3**
256×128	4 NC	619	215.9	1125	323.7	2839	734.9
256×128	2 NC	572	**172.2**	1055	**272.6**	2725	651.4
512×256	8	533	1453	1060	2469	2941	6112
512×256	8 NC	452	944.7	939	1673	2405	4229
512×256	8 NC-f	502	965.6	718	1290	1334	**2241**
512×256	4 NC	452	801.7	906	1359	2494	3456
512×256	2 NC	468	**746.6**	867	**1195**	2291	2770

Summary

- Developed a level-set approach for MHD
  - *The fixed boundary of the plasma in the poloidal plane is implicitly represented*
  - *The interior has a regular Cartesian mesh*
    - *No mapped grids, metric terms and coordinate singularities (advantage)*
    - *Mesh is not aligned with flux surfaces (disadvantage)*
  - *Boundary conditions imposed by extrapolation using PDEs and reflecting the normal components of velocity and the magnetic field*
- Simulated the motion of a localized high-density high-β region in 2D (axisymmetric) and 3D with AMR
  - *Instability triggered in short times after the formation of a local minimum in the toroidal field*
- 3D AMR HFS Pellet injection
  - *Parks electron heating model*
  - *High pressure annulus forms around the pellet due to electron heat flux*
- Developed a wave-structure based preconditioner for a Jacobian-Free Newton-Krylov method applied to MHD
  - *Preconditioner is exact for hyperbolic conservations laws in 1D*

Acknowledgement

- Phillip Colella, the Applied Numerical Algorithms Group, and the Applied Partial Differential Equations Center (APDEC) at Lawrence Berkeley National Laboratory

- Stephen C. Jardin & the Center for Extended MHD Modeling (CEMM) at the Princeton Plasma Physics Laboratory

- Daniel Reynolds (UCSD) and Carol Woodward (LLNL) - TOPS Center

- DOE SciDAC Program (Supported by US DOE Contract No. DE-AC020-76-CH03073)

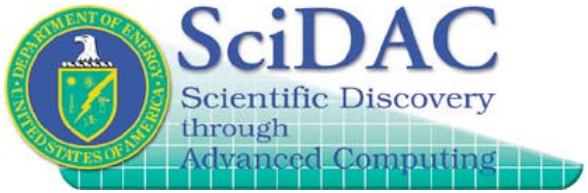

PPPL
PRINCETON PLASMA
PHYSICS LABORATORY